Small-Signal Characterization of Microwave and Millimeter-Wave HEMT's Based on a Physical Model

Ranjit Singh and Christopher M. Snowden, *Senior Member, IEEE*

Abstract— **A highly efficient generalized physics-based approach for small-signal characterization of FET devices is presented. A novel method is developed for extracting the frequency dependent two-port parameters from a single time-domain physical simulation based on a multi-signal excitation scheme. The technique is applied to simulating the frequency- and bias-dependent scattering parameters of HEMT's using a quasi-two-dimensional physical model that incorporates the main physical phenomena which govern the device behavior. A new carrier energy distribution model is presented which improves the accuracy of the physical model. An equivalent circuit is also generated from the physical dynamic simulation which can be used for predicting S-parameters and for indirect linking of the physical model to existing CAD tools. The unique formulation and efficiency of the present technique make it suitable for computer aided design of FET subsystems. The accuracy and flexibility of this approach is demonstrated by comparison of simulated results with measured data for a pulse doped pHEMT and uniformly doped GaAs channel HEMT.**

I. Introduction

SMALL-SIGNAL EQUIVALENT circuit models are widely used in CAE systems. Traditional small-signal HEMT models are based on equivalent circuits and the element values are determined from measurements by optimization of the fit to scattering (S)-parameters. The approach is particularly time consuming for efficiently modeling bias-dependent S-parameters and MMIC design. The elements values determined in this way lack a strong physical basis and the equivalent circuit models require extensive experimental data to establish a good basis of design and a large number of fitting coefficients. This approach is largely empirical and there is generally not a unique solution to the problem. Moreover, it is very difficult to characterize the effect of phenomena, such as DX centers and substrate trapping which are known to degrade the performance of the device. The physics-based model described in this paper is capable of efficiently modeling S-parameter bias dependence and provides a link between device, material, and process related parameters, and microwave performance. It enables the electrical performance to be considered at the device parameter level and makes the model highly suitable for MMIC design.

Manuscript received April 10, 1995; revised October 2, 1995.

The authors are with the Department of Electronic and Electrical Engineering, Microwave and Terahertz Technology Group, University of Leeds, Leeds, LS2 9JT, UK.

Publisher Item Identifier S 0018-9480(96)-00472-3.

This paper presents a computationally efficient physically based technique for simulating frequency-, amplitude-, and the bias-dependent S-parameters. At present there is a only a limited amount of published information available concerning physically-based small-signal S-parameter modeling of HEMT's, but there have been some developments [1]–[7], which have the potential to improve the capability of physically-based microwave and millimeter-wave CAD programs. Mahon *et al.* [8] reported a physically-based analytical technique for modeling HEMT structures by generating the core of a equivalent circuit from device material and geometric parameters, and a set of bias-independent parameters. The present work describes a generalized dynamic physical small-signal model in which a time domain physical simulation is directly included in the extraction schemes for S-parameters and physically-based equivalent circuit model elements. The specially developed multi-signal excitation scheme allows the extraction of frequency-dependent S-parameters and equivalent circuit element values from a single time domain simulation.

The basis of this work is a quasi-two-dimensional (Q2D) HEMT simulation [9], augmented with an avalanche breakdown model and improved energy distribution representation. The physical small-signal S-parameter scheme is used to characterize a pulse doped pHEMT and uniformly doped GaAs channel HEMT. It accurately predicts the S-parameters and provides the device performance prediction in terms of physical parameters without any fitting to measured data. The extracted equivalent circuit provides a indirect link between the physical modeling and existing CAD tools.

II. HEMT Physical Model

Physical models are predictive and produce results based on physical geometry, material, and carrier transport description of the device. The quasi-two-dimensional (Q2D) physical model used in the present work accounts for hot electron effects in submicron HEMT's, includes parasitic MESFET conduction, substrate injection, DX centers, and trapping phenomena. The basic principle of the model is described elsewhere [9] and the model structure is shown in Fig. 1. The model has been substantially improved incorporating an avalanche breakdown model and a improved carrier energy distribution representation. The semiconductor transport equations in each active layer of the device are solved

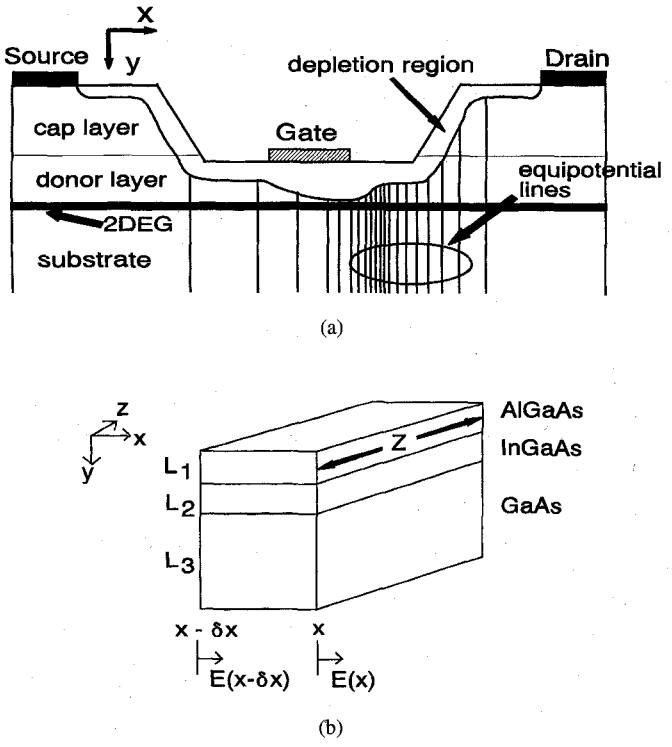

Fig. 1. (a) Quasi-two-dimensional HEMT model structure and (b) Gaussian surface under the gate in a pHEMT.

in a highly efficient manner with a self-consistent charge-control model [10]. The drain current is given by the sum of currents in all the active layers. In a conventional single channel HEMT there are three active layers; doped wide-band-gap, undoped smaller-band-gap and SI substrate layers. The equations governing the electron dynamics in each active layer of the device are

$$[E(x) - E(x-\delta x)]\, L_k - \delta E_{yk}(x)\, \delta x = \frac{Q_k}{\varepsilon_k} \quad \text{Gauss Law} \tag{1}$$

$$\frac{\partial J_k}{\partial x} + \frac{\partial \rho_k}{\partial t} = 0 \quad \text{Current Continuity} \tag{2}$$

$$\frac{\partial w_k}{\partial x} = \frac{3}{5}\left[qE(x) - \frac{w_k - w_o}{v_k \tau_k}\right] \quad \text{Energy Conservation} \tag{3}$$

$$v_k = \mu_k \left[E(x) - \frac{\partial w_k}{\partial x}\right] \quad \text{Momentum Continuity} \tag{4}$$

where L_k is the effective conductive height, Q_k is the net local charge and ε_k is the permittivity, J_k is the current density and p_k is the net local charge-density, μ_k is the electron mobility, v_k is the electron velocity, τ_k is the energy relaxation time for the kth layer, and δE_{yk} is the difference in electric field at the two boundaries of the kth layer. $E(x)$ is the longitudinal component of electric field and w_o is the lattice energy.

The model [9], which already incorporates the average energy dependent material parameters, has been substantially improved by incorporating the energy distribution of each

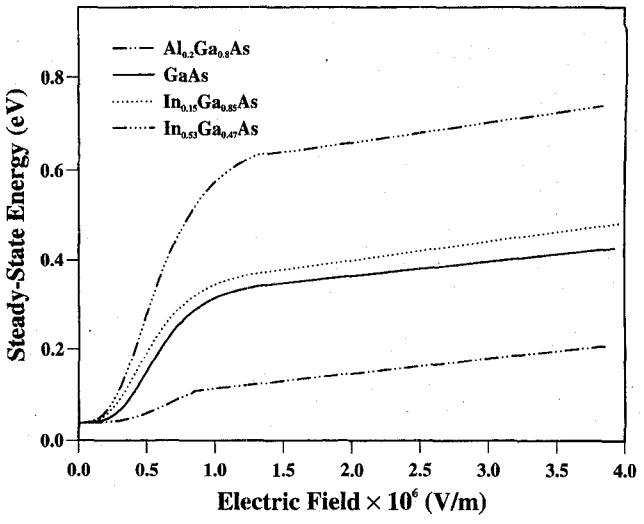

Fig. 2. Energy-electric field Monte Carlo characteristics for AlGaAs, GaAs, InGaAs.

active layer in to the transport parameters. The carrier energy distribution of two-dimensional electron gas (2DEG) is significantly different from those of doped layer and other active layers. A normalized stationary electric field model is incorporated. The energy distribution in each layer of the device is used to determine the corresponding steady state electric fields E_{ssk} from an energy-electric field characteristics obtained from that layer Monte Carlo simulations. These electric fields with corresponding carrier concentrations n_k in each layer are used to calculate the longitudinal stationary electric field $E_{ss}(x)$ as

$$E_{ss}(x) = \frac{\sum_k n_k E_{ssk}(w_k)}{\sum_k n_k}. \tag{5}$$

The energy-dependent mobility μ_k is then determined by relating the corresponding steady-state velocity v_{ssk} for the kth layer to the longitudinal stationary electric field and this yield the mobility μ_k as

$$\mu_k = \frac{v_{ssk}}{E_{ss}(x)}. \tag{6}$$

The steady-state electron energies and drift velocity versus electric field characteristics for AlGA's, GaAs, InGaAs material are shown in Figs. 2 and 3.

The present transport model assumes an equivalent single valley in a material. It is strictly true for a single-valley band structure material, such as silicon. This assumption is, however, reasonable in the present Q2D physical model since the transport and conservation equations are solved with the transport parameters generated from the Monte Carlo simulations. The multi-valley transfer effects and band non-parabolicity are simulated in the Monte Carlo calculations. The solution of full set of conservation equations facilitates the representation of the hot-electron effects and allow the model the capability of characterizing submicron gate length devices.

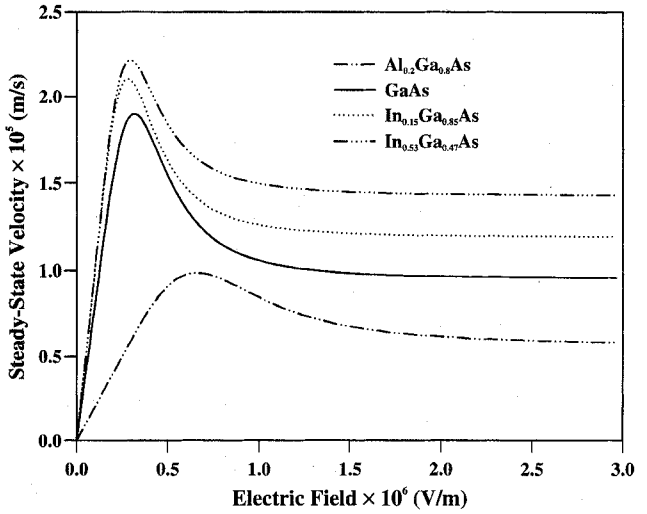

Fig. 3. Velocity-electric field Monte Carlo characteristics for AlGaAs, GaAs, InGaAs.

The model [9], which already accounts for gate current and contribution due to displacement current has been improved by incorporating avalanche breakdown model for gate and channel breakdown in the physical simulation. The model follows the work of Frensley [11], Wroblewski *et al.* [12], and Snowden and Pantoja [1]. Breakdown is assumed to occur when one of the following condition is satisfied

$$MF = 1 + \int_0^{l_{DS}} \alpha \, dx > 1 \quad \text{Channel Breakdown} \tag{7}$$

$$V_{DS} \geq V_{GDbr} - |V_{GS}| \quad \text{Gate Breakdown} \tag{8}$$

where l_{DS} is the drain-source spacing, MF is the multiplication factor and it expresses the ratio of the drain to source current, and channel breakdown occurs if MF significantly exceeds unity. The ionization rate α is expressed in terms of stationary electric field as

$$\alpha = C \exp\left\{-\left[\frac{E_c}{E_{ss}(x)}\right]^{\beta}\right\}. \tag{9}$$

Based on the work of Snowden and Pantoja [1] and model [12], the coefficients in the above equation have values

$$C = 1.8\,10^7\,\mathrm{m}^{-1},$$
$$E_c = 6.5 \times 10^7\,\mathrm{Vm}^{-1}$$

and

$$\beta = 2.$$

In gate breakdown condition, the voltage V_{GDbr} is given by

$$V_{GDbr} = \frac{2\varepsilon E_c^2}{C\sigma} \tag{10}$$

where ε is the permittivity and σ is the charge density.

III. Small-Signal Model

The physics-based small-signal characterization can be obtained by direct inclusion of a time-domain physical simulation in a S-parameter simulation scheme or by generating an equivalent circuit from the physical simulation. The simulation has also been used in large-signal design and analysis [4].

A. Dynamic Physical Model

The generalized technique for the physics based small-signal characterization of FET devices is described here. It is based on the concept introduced for the MESFET by Snowden and Pantoja [1]. At a large number of frequencies this approach is rather time consuming and a new modified technique is developed to suit CAD applications and presented here. Two port parameters are calculated in two stages. Firstly, the output (drain-source) port is driven with a mixed multi-signal sinusoidal source current i_{S1}, superimposed on DC bias I_S, and given by

$$i_{S1} = I_S + \sum_i I_{SRF} \sin(2\pi f_i t) \tag{11}$$

where I_{SRF} is the amplitude of RF component of sinusoidal source current and summation is across the whole range of frequencies of interest at which small-signal S-parameters are to be evaluated (note that I_{SRF} must be sufficiently small to maintain linearity). The input (gate-source) port is short circuited for RF signals. The simulation is allowed to run several cycles to allow transients effects to settle down. The gate- and drain-current and drain-source voltage waveforms are calculated from the Q2D physical simulation. The discrete Fourier Transformation of all the waveforms gives phasors $I_{G1}(\omega)$, $I_{D1}(\omega)$, $V_{DS1}(\omega)$, for simulating frequency and its harmonics. The multi-frequency problem is transformed to an equivalent single frequency by choosing the simulating frequency to be highest common factor of all the frequencies such that all the frequencies of interest are an integral multiple of the simulating frequency. The admittance (Y)-parameters $Y_{12}(\omega)$ and $Y_{22}(\omega)$, at a frequency ω are determined by

$$Y_{12}(\omega) = \frac{I_{G1}(\omega)}{V_{DS1}(\omega)} \tag{12}$$

$$Y_{22}(\omega) = \frac{I_{D1}(\omega)}{V_{DS1}(\omega)}. \tag{13}$$

In the second stage, the input-port is driven with a mixed multi-signal sinusoidal voltage v_{GS1}, superimposed on the DC bias V_{GS}, and given by

$$v_{GS1} = V_{GS} + \sum_i V_{GRF} \sin(2\pi f_i t) \tag{14}$$

where V_{GRF} is the amplitude of the RF component gate voltage. The output port is held open short circuit for RF signals. The gate-current and drain-source voltage waveforms are calculated and after Fourier Transformation this then gives

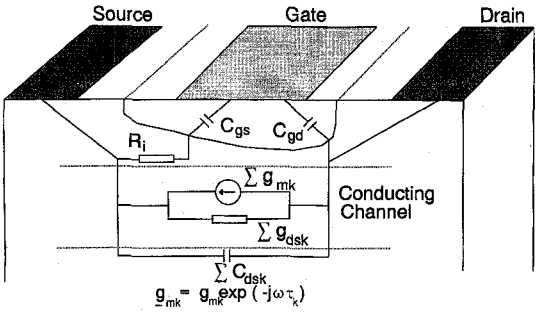

Fig. 4. Physical basis of HEMT small-signal circuit model.

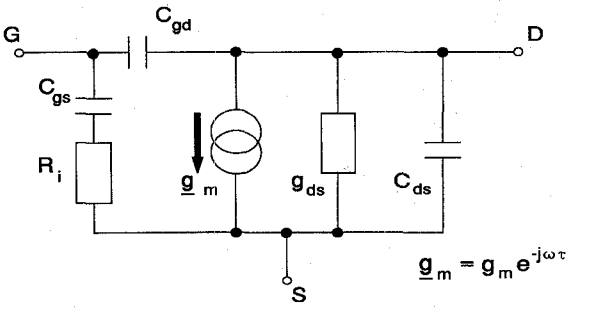

Fig. 5. Topology of intrinsic small-signal circuit based on physical model.

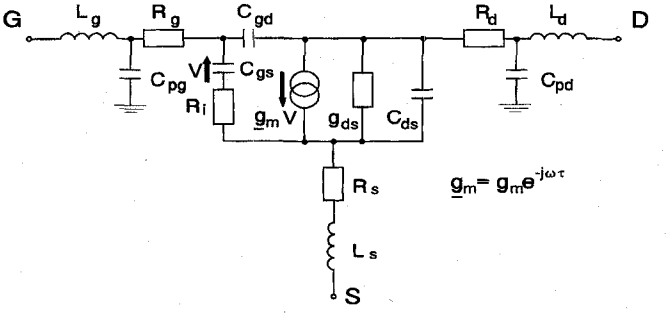

Fig. 6. Topology of small-signal circuit with parasitics.

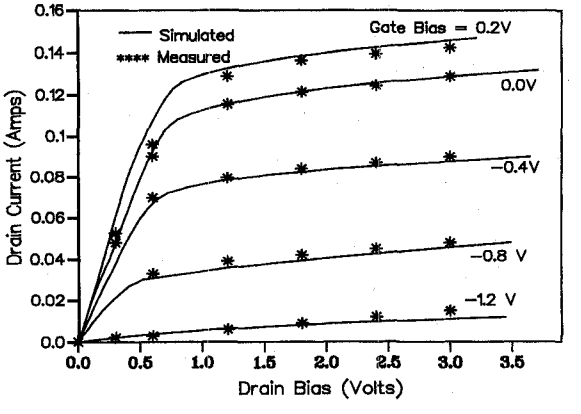

Fig. 7. Measured and simulated DC characteristics of the pHEMT.

$Y_{11}(\omega)$ and $Y_{21}(\omega)$

$$Y_{11}(\omega) = \frac{I_{G2}(\omega) - Y_{12}(\omega)V_{DS2}(\omega)}{V_{GS2}(\omega)} \tag{15}$$

$$Y_{21}(\omega) = \frac{I_{D2}(\omega) - Y_{22}(\omega)V_{DS2}(\omega)}{V_{GS2}(\omega)}. \tag{16}$$

This technique produces the admittance-parameters of the intrinsic device for all the frequencies at the same time. The parasitic impedances can be added to intrinsic admittance-parameters and the corresponding S-parameters are obtained by $Y \rightarrow S$ conversion formulas. Maximum available gain, Rollet stability factor and other related parameters in subsystem design can also be evaluated. The amplitude of the exciting waveforms must be chosen to ensure linear and noise free results. A key feature of this technique is that it is possible to relate physical and geometrical changes in the device design to changes in the performance. It enables a wide range of process parameter variation to be investigated in a very short time without resorting to fabrication experiments.

B. Physics-Based Equivalent Circuit Model

The equivalent circuit models are popular with practicing engineers and in some circumstances offer a speed advantage over a full implementation of the physical model. An equivalent circuit model generated from the physical simulation is presented here. The physical basis of the HEMT equivalent circuit is shown in Fig. 4. In a HEMT, the conductive channel is controlled by the Schottky barrier gate potential and intrinsic gain is provided by the device transconductance, g_m. The conductive channel in a HEMT is the combination of multilayer conduction paths possible within the device structure. The gate voltage simultaneously changes the carrier concentrations present in several regions with different transport properties. The multilayer conduction path make the equivalent circuit problem more involved as this phenomena is bias dependent. The device g_m is a combination of all the conducting regions transconductances (Σg_{mk}). The transit time constant, τ represents the time taken by carriers to travel under the effective gate region, either side of the gate. The effective gate length is distance between the edges of the gate depletion depth. The device output conductance, g_{ds} is a measure of the incremental change in the output current I_{DS} versus output voltage V_{DS}, while the input voltage V_{GS} is held constant. It is combination of multilayer conductances (Σg_{dsk}). The input gate capacitance is dependent on the depletion region under the gate and channel carrier concentration, which depends on the gate voltage and lateral channel potential. It is distributed and resistively connected to the conducting channel. The input gate-source network can be represented by a distributed series combination of capacitance C_{gs} and resistance R_i. The gate-drain capacitance, C_{gd} represent a feedback path between the drain and gate due to coupling between gate-drain. It is distributed and is connected to low resistivity conducting channel. The drain-source capacitance C_{ds} is also associated with multilayer conduction paths within the device.

The basic HEMT can be represented by a small-signal circuit model without parasitics as shown in Fig. 5. The core of the model is directly dependent on the process-oriented technological parameters and accurately predicts the bias-dependent S-parameters. It does not require fitting coefficients. An important feature of this equivalent circuit model is that all the elements are nonlinear (bias-dependency is intrinsically available from the Q2D model). Equivalent circuit model

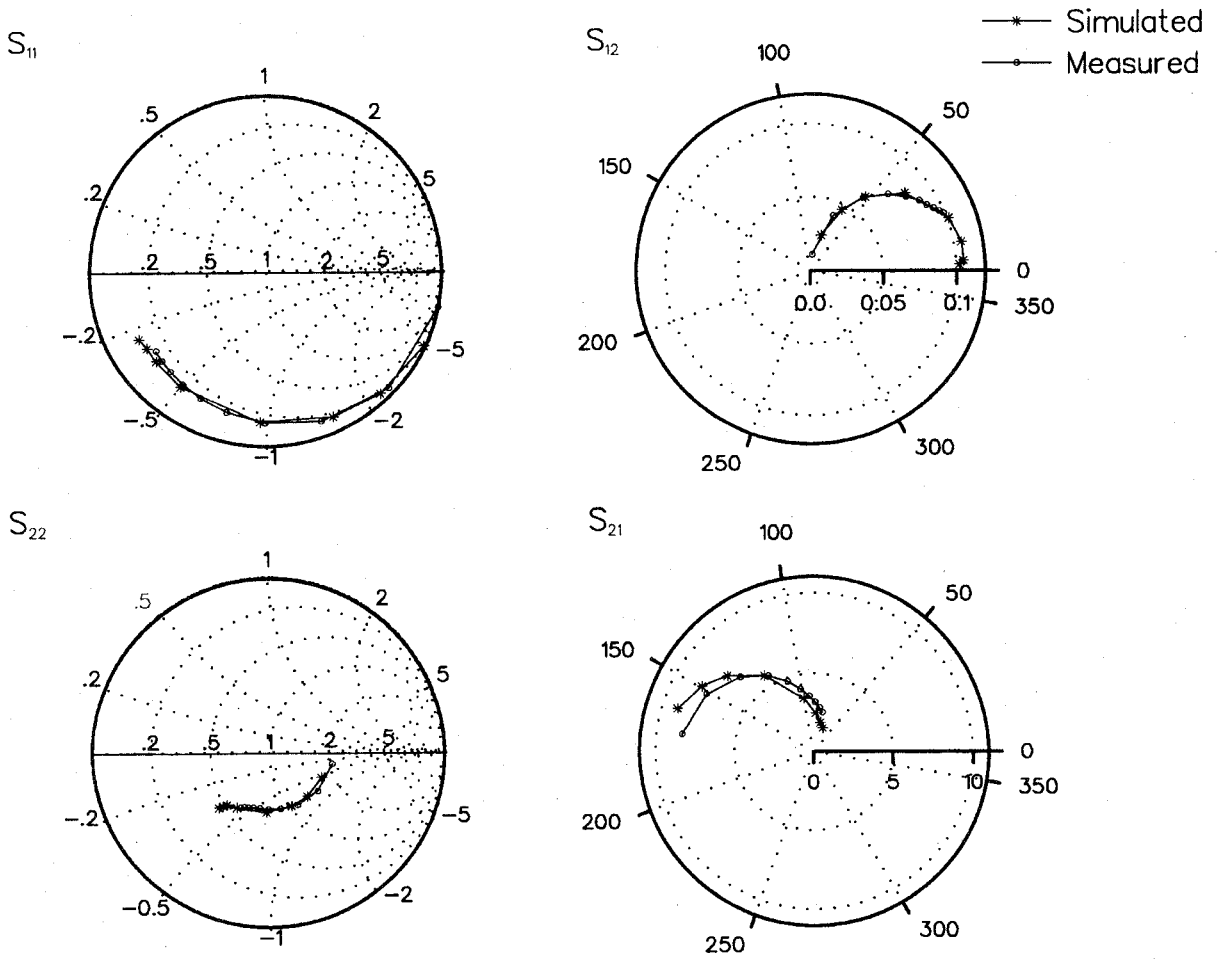

Fig. 8. Small-signal scattering parameters of the pHEMT.

elements are extracted by generating the frequency-dependent Y-parameters of the intrinsic device using the two-stage multi-signal excitation based on the physical approach described above. The intrinsic circuit model has seven element values and these can be expressed in term of Y-parameters as

$$C_{gd}(\omega) = \frac{-\mathrm{Im}\,[Y_{12}(\omega)]}{\omega} \tag{17}$$

$$C_{gs}(\omega) = \frac{\mathrm{Im}\,[Y_{11}(\omega)] - \omega C_{gd}(\omega)}{\omega} \cdot \left\{1 + \frac{\mathrm{Re}\,[Y_{11}(\omega)]^2}{\{\mathrm{Im}\,[Y_{11}(\omega)] - \omega C_{gd}(\omega)\}^2}\right\} \tag{18}$$

$$R_i(\omega) = \frac{\mathrm{Re}\,[Y_{11}(\omega)]}{\{\mathrm{Im}\,[Y_{11}(\omega)] - \omega C_{gd}(\omega)\}^2 + \{\mathrm{Re}\,[Y_{11}(\omega)]\}^2} \tag{19}$$

$$g_m(f) = \sqrt{\begin{array}{l}\{\mathrm{Re}\,[Y_{21}(\omega)]\}^2 \\ \quad +\{\mathrm{Im}\,[Y_{21}(\omega)] + \omega C_{gd}(\omega)\}^2 \\ \quad \cdot[1 + \omega^2 C_{gs}^2(\omega) R_i^2(\omega)]\end{array}} \tag{20}$$

$$\tau(\omega) = \frac{1}{\omega}\arcsin\{-\mathrm{Im}\,[Y_{21}(\omega)] - \omega C_{gd}(\omega) - \omega C_{gs}(\omega) R_i(\omega)\,\mathrm{Re}\,(Y_{21})\} \tag{21}$$

$$C_{ds}(\omega) = \frac{\mathrm{Im}\,[Y_{22}(\omega)] - \omega C_{gd}(\omega)}{\omega} \tag{22}$$

$$g_{ds}(\omega) = \mathrm{Re}\,[Y_{22}(\omega)] \tag{23}$$

where ω is the angular frequency. The parasitic impedances at the gate, source, and drain contacts are added as circuit elements as shown in Fig. 6. The scattering parameters are then calculated from the elements of the model. The present technique allows accurate extraction of physical equivalent circuit for a wide variety of FET structures and makes the simulation ideal for incorporating into circuit models. The accuracy of the model presented here relies on the original physical simulation which relates the circuit elements to the physical operation. It is valid at the higher frequencies, where the multilayer conduction and displacement currents are taken into consideration in the dynamic physical formulation based on the time-domain transport equations.

The circuit model element values remain constant over a considerable frequency range. The S-parameters over this frequency range can be calculated by extracting the circuit element values corresponding to a single frequency. The multi-frequency technique described above, however, allows the frequency-dependent element values to be evaluated from frequency-dependent Y-parameters provided by single time-domain simulation at the equivalent transformed frequency.

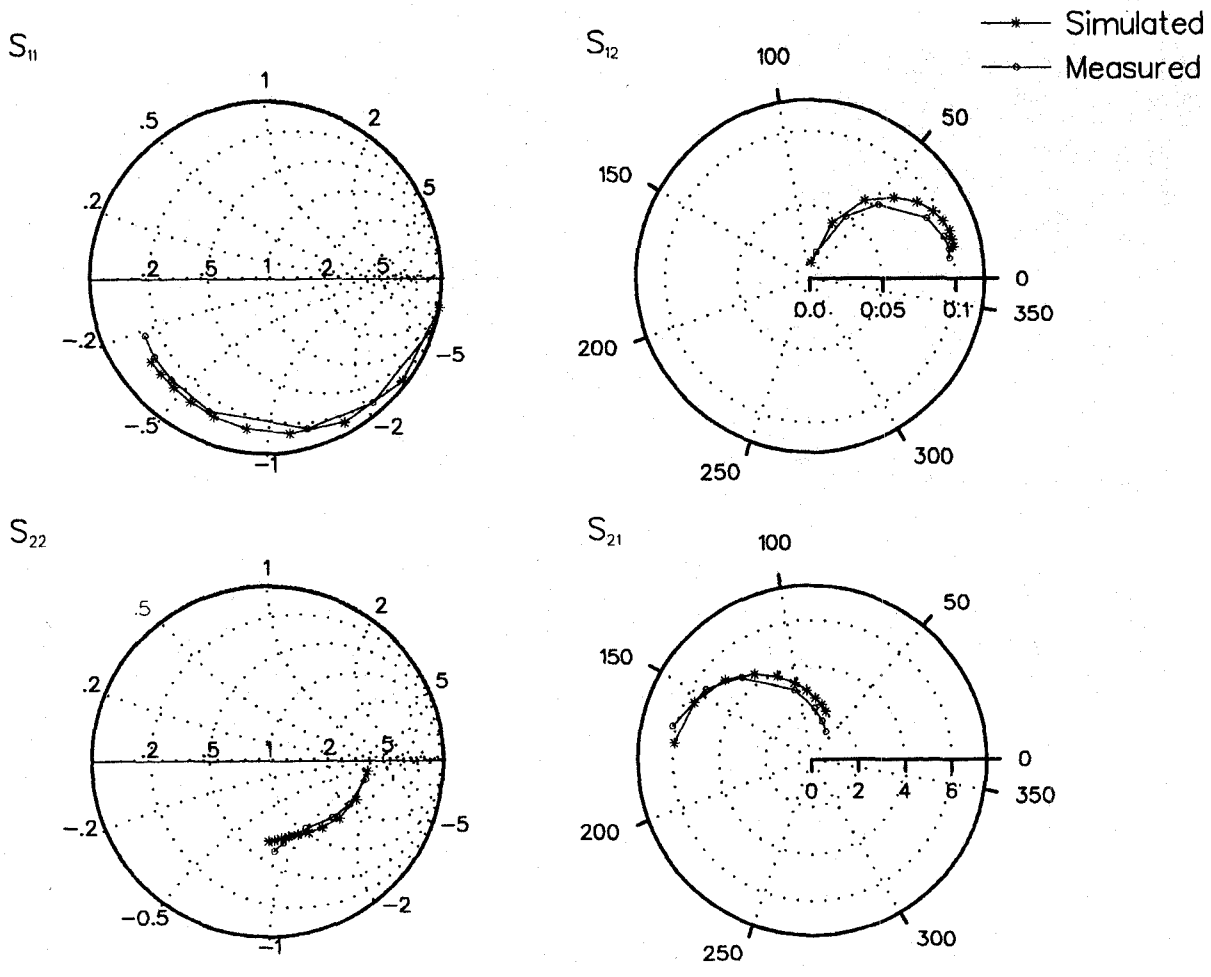

Fig. 9. Small-signal scattering parameters of the AlGaAs/GaAs HEMT.

IV. Results and Discussion

A pulse-doped AlGaAs/InGaAs/GaAs pHEMT and uniformly-doped AlGaAs/GaAs HEMT devices have been simulated to validate the approach. The measured and simulated DC characteristics of a 0.25 μm pulse-doped pHEMT with gate width of 300 μm are shown in Fig. 7 and the small-signal S-parameters over the frequency range 1.0–26.0 GHz at $V_{DS} = 2.0$ V, $V_{GS} = -0.65$ V are shown in Fig. 8. The measured and simulated small-signal S-parameters of 0.25 μm AlGaAs/GaAs HEMT over the frequency range 1.0–26.0 GHz at $V_{DS} = 2.0$ V, $V_{GS} = 0.0$ V are shown in Fig. 9. The measured data was obtained using a wafer-probe technique. The simulated results have been determined using the physical data and parasitic inductance element values extracted from the on wafer calibration and *no further fitting* is performed. The model make use of parasitic resistances and capacitances calculated during the physical simulation, which includes the contact and access resistances and interelectrode capacitances. The level of agreement between modeled and measured RF results can be improved to achieve an excellent level of fit by adjusting the extrinsic parasitic element values, but this was not the aim of the work, which was to demonstrate the predictive capability of the model. Fig. 10 shows the bias-dependent intrinsic equivalent circuit element values extracted from a series of dynamic physical simulations.

The Q2D dynamic simulation provides the results in the form of time domain waveforms. The amplitude of the exciting signals must be large enough to provide the numerical noise free results and sufficiently small to ensure linear operation without intermodulation. Typically, RF gate voltage amplitudes 0.1–1 mV and RF source current amplitudes 0.05–0.5 mA are used. The specially developed two-stage technique for Y-parameters calculation is more efficient and suitable for CAD due to ability to predict the frequency dependent Y-parameters from a single time domain simulation and has no iterative method. The typical CPU time for a full multi-frequency S-parameter simulation scheme at one bias point is about a minute on a SUN LPX SPARC workstation. The present approach produces the true AC quantities and accounts for bias-dependent multi-conduction paths, distributed phenomena, and deep-level effects occurring in the device.

V. Conclusion

A highly efficient generalized physically-based S-parameter extraction scheme is described. It is easily applied to MESFET and a wide variety of HEMT structures. Application of

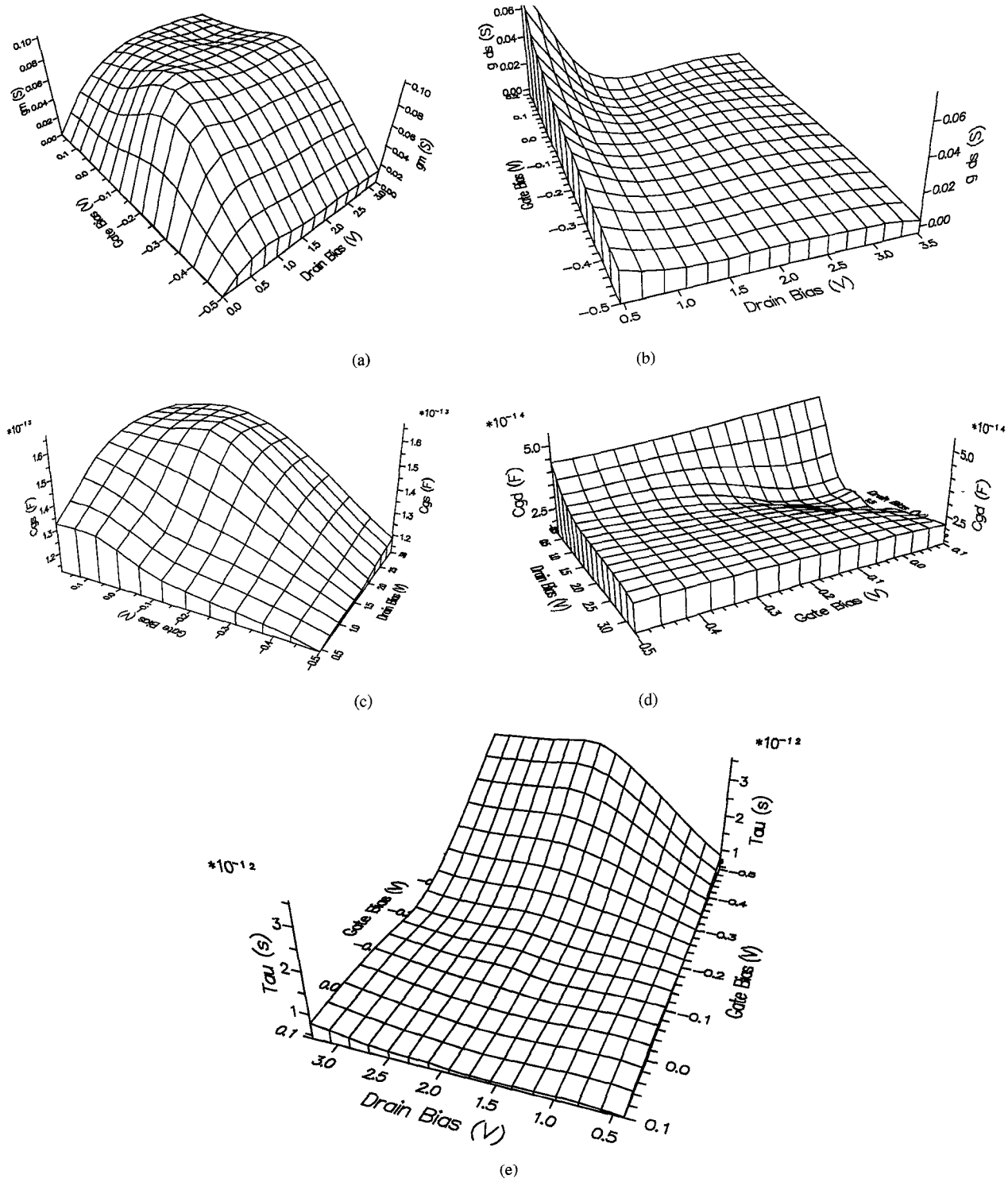

Fig. 10. Variation of equivalent circuit parameters with gate and drain biases; (a) transconductance; (b) output conductance; (c) gate-source capacitance; (d) gate-drain capacitance; and (e) transit time-constant.

the multifrequency excitation concept in the small-signal S-parameter extraction scheme, drastically reduces the complexity of the multi-frequency simulation problem by transforming it to an equivalent single-signal case. The HEMT simulator incorporated in the scheme accounts for hot electron effects in submicron HEMT's, parasitic MESFET conduction, substrate injection, quantum, and deep level effects. A new carrier-distribution model has been incorporated into the physical simulation. It improves the accuracy by incorporating the energy distribution of each active layer in the transport parameters.

A physical equivalent circuit model is presented. The equivalent circuit elements are derived from dynamic physical simulation with a high degree of computational efficiency. The

present technique allows the investigation of the frequency, signal-level, and bias dependency of RF parameters starting from the process-oriented technological stage and thereby making the present work suitable for MMIC CAD. Results obtained from the actual devices have shown close agreement between predicted and measured results.

ACKNOWLEDGMENT

The authors would like to acknowledge the stimulatory discussions with R. Drury, J. S. Atherton, and the members of Microwave and Terahertz Technology Group at Leeds.

REFERENCES

[1] C. M. Snowden and R. R. Pantoja, "Quasi-two-dimensional MESFET simulation for CAD," *IEEE Trans. Electron Devices,* vol. 36, no. 9, pp. 1564–1574, 1989.

[2] ——, "GaAs MESFET physical model for process-oriented design," *IEEE Trans. Microwave Theory and Tech.,* vol. 40, no. 7, pp. 1401–1409, July 1992.

[3] R. R. Pantoja, M. J. Howes, R. R. Richardson, and C. M. Snowden, "A Large-signal physical MESFET model for computer-aided design and its applications," *IEEE Trans. Microwave Theory Tech.,* vol. 37, no. 12, pp. 2039–2045, Dec. 1989.

[4] R. Singh and C. M. Snowden, "Large-signal modeling of millimeterwave HEMT's," in *Proc. 24th European Microwave Conf.,* Cannes, 1994, pp. 1325–1330.

[5] G. Ghione, C. U. Naldi, and F. Filicori, "Physical modeling of GaAs MESFET's in an integrated CAD environment: from device technology to microwave circuit performance," *IEEE Trans. Microwave Theory Tech.,* vol. 37, no. 3, pp. 457–468, Mar. 1989.

[6] F. Filicori, G. Ghione, and C. U. Naldi, "Physics-based electron device modeling and computer-aided MMIC design," *IEEE Trans. Microwave Theory Tech.,* vol. 40, no. 7, pp. 1333–1352, July 1992.

[7] J. W. Bandler, R. M. Biernacki, Q. Cai, S. H. Chen, S. Ye, and Q. Zhang, "Integrated physics-oriented statistical modeling, simulation and optimization," *IEEE Trans. Microwave Theory Tech.,* vol. 40, no. 7, pp. 1374–1400, July 1992.

[8] S. J. Mahon, D. J. Skellern, and F. Green, "A technique for modeling S-parameters for HEMT structures as a function of gate bias," *IEEE Trans. Microwave Theory Tech.,* vol. 40, no. 7, pp. 2336–2344, July 1992.

[9] R. Singh and C. M. Snowden, "A quasi-two-dimensional HEMT model for DC & microwave simulation incorporating deep level effects," Submitted for publication in *IEEE Trans Electron Devices.*

[10] ——, "A self-consistent charge-control model for HEMT's incorporating deep level effects," in *Proc. Int. Workshop on Computational Electronics,* Leeds, 1993, pp. 60–64.

[11] W. R. Frensley, "Power-limiting breakdown effects in GaAs MESFET's," *IEEE Trans. Electron Devices,* vol. 28, no. 8, pp. 962–970, Aug. 1981.

[12] R. Wroblewski, G. Salmer, and Y. Crosnier, "Theoretical analysis of the DC avalanche breakdown in GaAs MESFET's," *IEEE Trans. Electron Devices,* vol. 30, no. 2, pp. 154–159, Feb. 1983.

[13] M. Berroth and R. Bosch, "Broad-band determination of the FET small-signal equivalent circuit," *IEEE Trans. Microwave Theory Tech.,* vol. 38, no. 7, pp. 891–895, July 1990.

Ranjit Singh was born in New Delhi, India on February 24, 1963. He received the B.Sc., M.Sc., and M. Tech. degrees from the University of Delhi in 1983, 1985, and 1987, respectively.

He joined the Microwave Group in the National Physical Laboratory, New Delhi in 1987, where he is currently holds the position of Scientist. During the period 1992 to 1995, he was on a Commonwealth Fellowship in the Microwave and Terahertz Technology Group at the University of Leeds, where he carried out research work leading to Ph.D. degree, on characterization and modeling of various HEMT structures. His main research interests include microwave/millimeterwave measurements, semiconductor devices, and microstrip antenna modeling and nonlinear circuit design.

Dr. Singh was awarded Science Meritorious Award and Certificate of Merit from the University of Delhi in 1985, and 1987, respectively. He was an Invited Scientist at the XXIV General Assembly of URSI in the Young Scientist Award Scheme.

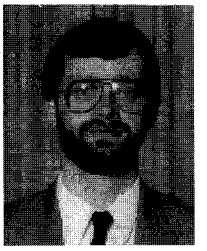

Christopher M. Snowden (S'82-M'82-SM'91) received the B.Sc., M.Sc., and Ph.D. degrees from the University of Leeds.

After graduating in 1977, he worked as an Application Engineer for Mullard, Mitcham. His Ph.D. studies were conducted in association with Rascal-MESL and were concerned with the large-signal characterization of MESFET microwave oscillators. In 1982, he was appointed Lecturer in the Department of Electronics at the University of York. He joined the Microwave Solid State Group in the Department of Electronic and Electrical Engineering at the University of Leeds in 1983, where he currently hold the Chair of Microwave Engineering. He is also Head of Department of Electronic and Electrical Engineering at the University of Leeds. During 1987, he was a Visiting Research Associate at California Institute of Technology. He has been a consultant to M/A-COM Inc., Corporate Research and Development since 1989, where he was on sabbatical leave during the period 1990 to 1991. During this year, he represented M/A-COM as Senior Staff Scientist. His main research interests include compound semiconductor device modeling, microwave, terahertz and optical nonlinear subsystem design, and advanced semiconductor devices. He has written seven books and more than 135 papers.

Dr. Snowden is the chairman of 1995 International Microwaves and RF Conference. He is a Member of the MTT Electromagnetic Academy and a Fellow of the IEE. He is a founding member of the International GaAs Simulation Group.